J Mater Sci (2010) 45:2598–2605
DOI 10.1007/s10853-010-4233-x

Influence of crystallographic textures on tensile properties of 316L austenitic stainless steel

B. Ravi Kumar

Received: 6 April 2009 / Accepted: 11 January 2010 / Published online: 26 January 2010

Abstract Role of cold rolling texture on the tensile properties of the cold rolled and cold rolled and annealed AISI 316L austenitic stainless steel is described here. The solution-annealed stainless steel plates were unidirectionally cold rolled to 50, 70 and 90% of reduction in thickness. The cold rolled material was annealed at 500–900 °C annealing temperatures. X-ray diffraction technique was employed to study the texture evolution in cold rolled as well as cold rolled and annealed conditions. The texture components that evolved were translated into slip transmission number 'λ' and Schmid factor 'μ'. These two parameters were correlated with the tensile properties of the material. The tensile properties were evaluated under all processing conditions. Softening of the cold rolled material was observed after annealing with increasing annealing temperatures. From the stress–strain curves, strain hardening coefficient 'n' and strain hardening rate 'θ' were determined. It was found that the effect of texture on tensile behaviour could be understood clearly by strain hardening rate. Out of the two parameters, 'n' and 'θ', strain hardening rate was found to be more sensitive to type of texture in the material.

Introduction

Performance of polycrystalline materials is linked to microstructural features such as microstructural heterogeneities and/or boundaries. The microstructural heterogeneities are expected to influence the behaviour of the material during plastic deformation. Apart from grain boundaries and phase boundaries, lattice misorientation at grain boundaries as well as within them plays a prominent role. The orientation relationship between neighbouring grains determines the efficiency of grain boundaries as an obstacle to dislocation motion [1–3]. During deformation, dislocations have to move from one grain to another. The transfer of dislocations across the grain through the grain boundary is an important step in controlling the deformation behaviour/flow stress of the material. The effect of grain boundaries can be realized from the Hall–Petch relations. Depending on the nature of the grain boundaries, the slope of the Hall–Petch curve can increase or decrease. Furthermore, on macroscopic scale, orientation distribution, i.e. the orientation relationship between the grains and its neighbouring grains representing crystallographic texture of a polycrystalline material also influences the deformation behaviour. Therefore, the nature of the microstructure and texture reflects on the plastic deformation behaviour of the materials which determine the mechanical properties. However, in order to evaluate the contribution from the deformation texture to the microstructure dependence of yield strength, it is necessary to eliminate the deformation microstructure dependence from yield strength of the material.

In view of the above, for studying the effect of texture on mechanical properties, two of the important parameters that are affected by texture were investigated. The first parameter studied was the well-known effect of Schmid factor (μ)

$$\tau = \sigma \cdot \cos\phi \cdot \cos\lambda = \sigma \cdot \mu \quad (1)$$

which can influence the overall deformation behaviour of the material [4, 5]. In Eq. 1, 'ϕ' is the angle between the slip plane normal and the tensile stress direction, and 'λ' is

B. Ravi Kumar (✉)
Materials Science and Technology Division, National Metallurgical Laboratory, CSIR, Jamshedpur, India
e-mail: ravik_in@yahoo.com; ravik@nmlindia.org

the angle between the slip direction and the tensile axis. A preferential orientation of the grains due to crystallographic texture may result towards high Schmid values. High 'μ' value is a preferable condition for the plastic deformation of grains in the applied stress direction. A large fraction of grains with high value of 'μ' probably assist simultaneous operation of multiple slip systems and exhibit high strain hardening rate [4].

The second parameter related to the influence of texture on the grain boundaries was correlated to the ease of slip transfer as predicted by Werner and Prantl [6]. The model predicts a slip transfer number λ as follows:

$$\lambda = \sum_{i=1}^{144} \left[\cos\left(\frac{90^\circ}{\varepsilon_c} \cdot \varepsilon_i \right) \cdot \cos\left(\frac{90^\circ}{\kappa_c} \cdot \kappa_i \right) \right] \quad (2)$$

where ε is the angle between the interacting slip plane normal and κ is the angle between the slip directions. Both ε_i and κ_i must satisfy their limiting conditions $\varepsilon_i < \varepsilon_c$ and $\kappa_i < \kappa_c$, respectively. The above equation predicts that the higher the 'λ' value, the easier the slip transfer across the boundaries. Depending on the efficacy of the slip transfer across the grain boundaries, the tensile properties are expected to vary [2, 7].

In this investigation, single fcc austenite phase stainless steel (ASS) was cold rolled and annealed in order to understand the contribution of texture on tensile properties. This was correlated with simultaneous changes occurring in the deformed microstructure. The results are used as a base to evaluate the influence of cold deformation texture on the stainless steels, which are subjected to thermo-mechanical processes.

Experimental

The as-received austenitic stainless steels in the form of 10-mm thick plates were solution treated at 1080 °C for 1 h and quenched in water to achieve chemical homogeneity. The specimens were then rolled at room temperature for thickness reduction up to 50, 70 and 90% in a two-high rolling mill under oil lubrication. The multipass unidirectional cold rolling with constant thickness reduction at each pass was performed to achieve desired thickness reduction. Cold rolled material was annealed at various temperatures ranging from 500 to 1000 °C for 1 h in a muffle furnace.

Microstructural examination of the cold rolled and aged specimens after different rolling reductions was carried out by standard metallographic techniques. A mixture of three parts of HCl and one part of HNO_3 was used to reveal the microstructure for optical microscopy. The texture was measured by the conventional Schultz reflection technique [8] using X-ray diffraction. Three incomplete pole figures for the (200), (220) and (311) reflection for the austenite phase were recorded using Mo Kα radiation by Seifert XRD 3003 PTS diffractometer. Experimental pole figure data were used to calculate orientation distribution function (ODF) plots using LaboTex software, developed by LaboSoft s.c., Poland [9, 10].

25-mm gauge length flat tensile specimens were machined from the specimen blanks in as-received, cold rolled and aged conditions. All the specimens were prepared with their loading axis parallel to the rolling direction. Tensile tests were conducted, as per ASTM standard E-8M, at room temperature under displacement control at a rate of 0.2 mm/min using Instron 8501 closed loop servo-hydraulic dynamic testing system of 100 kN capacity equipped with model 8500 digital controller. Elongation was measured by an extensometer of 25-mm gauge length. 0.2% offset method was followed to arrive at the yield strength.

Results and discussion

Microstructural changes

Microstructural studies of the solution-annealed material exhibited polygonal grain features as shown in Fig. 1. Cold rolling resulted in the formation of elongated grain structure in the rolling direction (RD). A very stable deformed microstructure was retained even after annealing up to 700 °C for all the cold rolling conditions. Figure 2 shows typical microstructures of 90% cold rolled and annealed ASS at different annealing temperatures. From the microstructure, it was observed that the deformed structure did

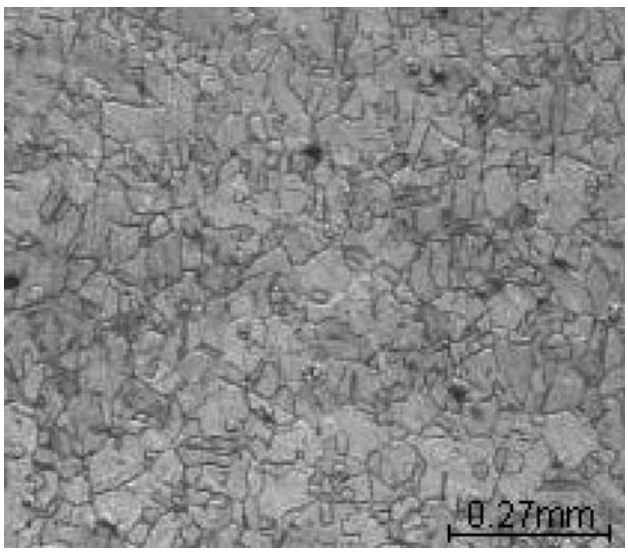

Fig. 1 Microstructures of austenitic 316L SS revealing polygonal grain features after solution anneal treatment

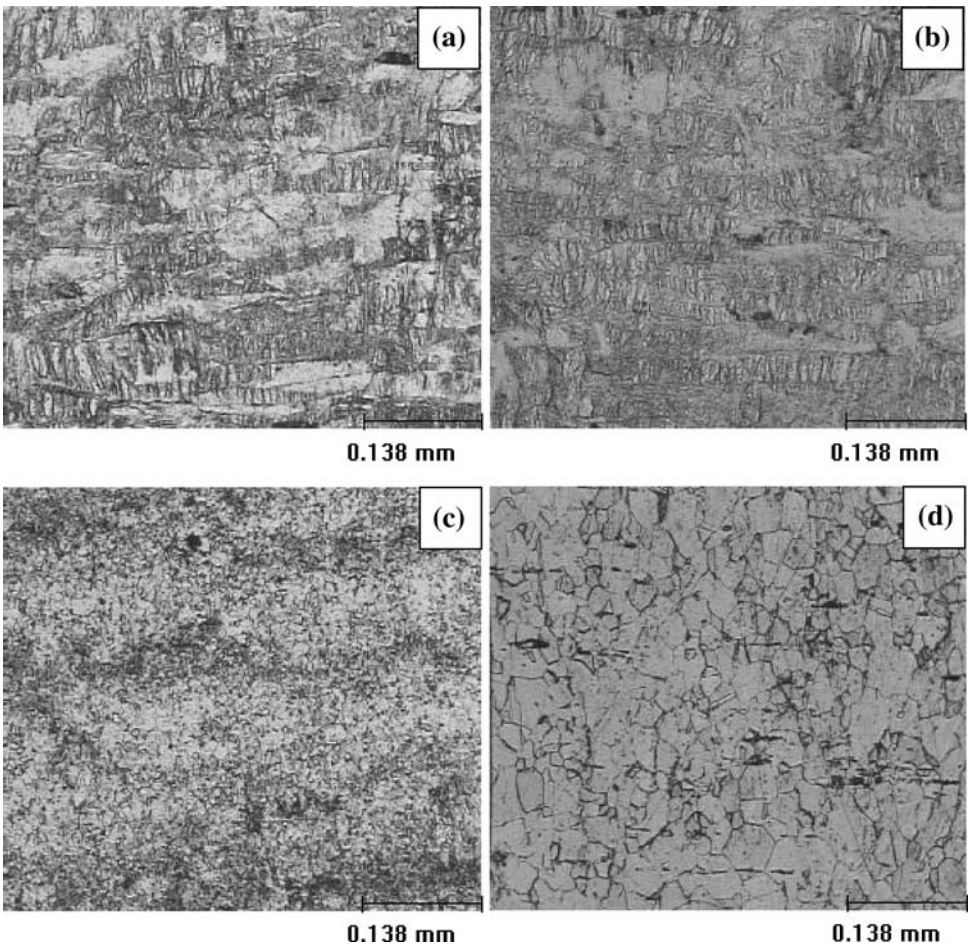

Fig. 2 Microstructure of the 90% cold rolled and annealed 316L ASS showing recovery of some deformed grain **a** at 600 °C, **b** at 700 °C, **c** recrystallization with very fine grain size at 900 °C, **d** grain growth at 1000 °C

not undergo any major recovery process even at the annealing temperature of 700 °C. However, annealing at and above 900 °C resulted in recrystallized microstructure. A very fine grain microstructure was observed for all the specimens annealed at 900 °C. Further, increase in annealing temperature resulted in grain growth.

Evolution of texture

Figure 3 shows the typical ODF plots of constant ϕ_2-sections-fibre texture, showing the development of preferred orientations by cold rolling. The textures developed in fcc materials are typically characterized by β-fibre [11–13], consisting of $\{112\}\langle 111\rangle$ Cu, $\{123\}\langle 643\rangle$S and $\{011\}\langle 211\rangle$B orientations. The volume fractions of these important fcc texture components are shown in Fig. 4. With increasing cold rolling reduction in thickness, changes in texture characteristics can be noted from Fig. 4. 50% of cold rolling of ASS revealed very strong B texture component. As the % of cold rolling increased, development of S and G texture components was observed. Annealing of cold rolled ASS did not produce any perceptible change in the β-fibre even up to the annealing temperature of 900 °C, indicating stable texture condition. From microstructural investigation, it was noted that the cold deformed structure fully recrystallized at an annealing temperature of 900 °C. In this study, even after the full recrystallization of the deformed structure, the intensity of the main cold rolling texture components was observed to remain same. The volume fraction of B orientation was found to show decreasing trend in specimen's cold rolled to 50% with increasing annealing temperature. In the case of 70% cold rolled and annealed specimen, texture components showed decrease in B and S orientations with stable G orientation (Fig. 4). On the other hand, 90% cold rolled specimens showed very stable B and G components with an appreciable decrease in S component. The retention of cold rolling textures was attributed to the solute effect of molybdenum present in the 316L SS by Donadille et al. [14].

Mechanical properties

Results of the tensile test are presented in Table 1. Figure 5 shows the tensile true stress–strain curve for cold rolled and annealed specimen. Annealing at 500 °C did not bring any change in the properties from the cold rolled condition. However, annealing above 500 and up to 700 °C resulted

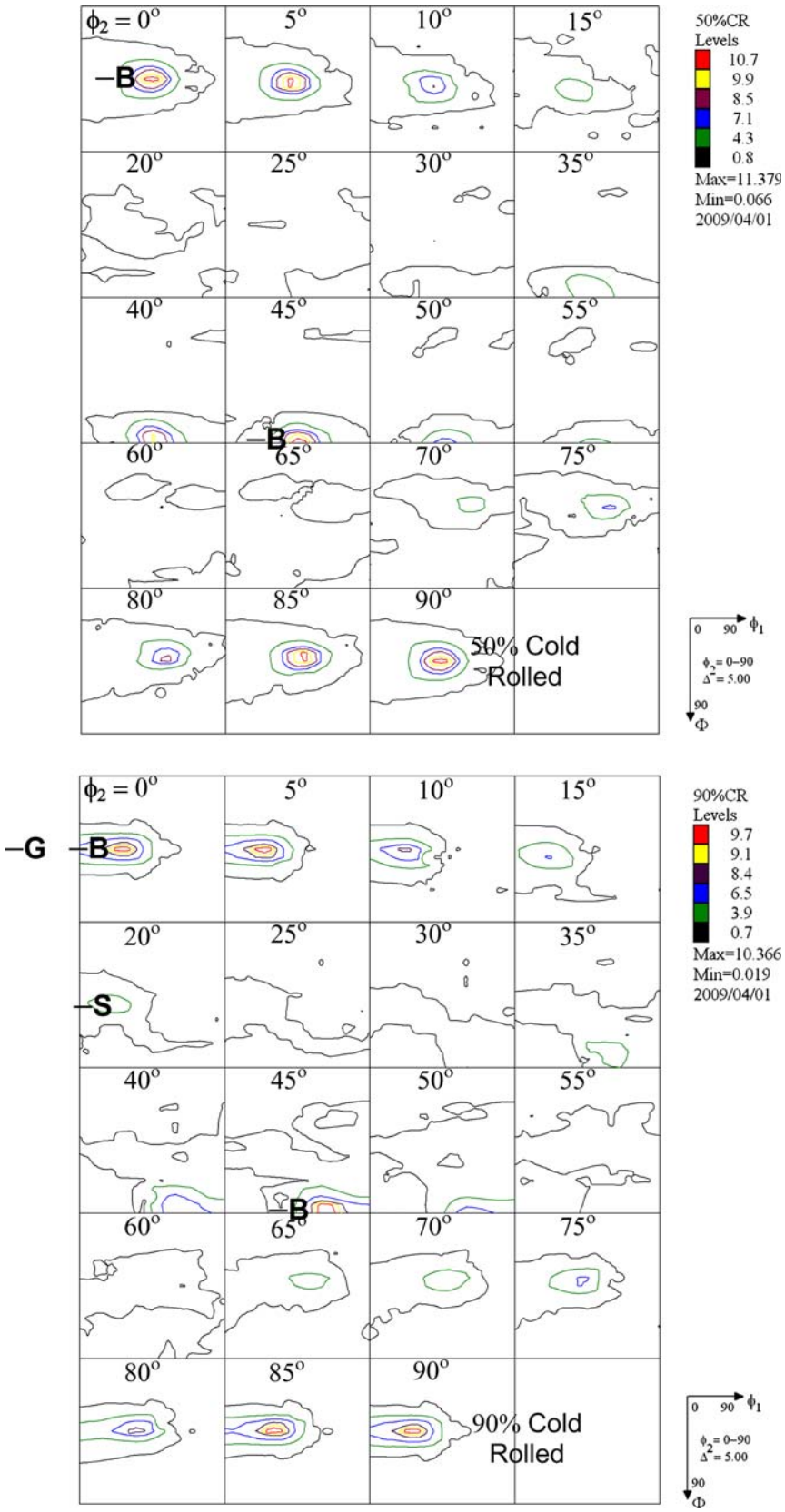

Fig. 3 ODF of 50 and 90% cold rolled 316L ASS showing ideal texture components

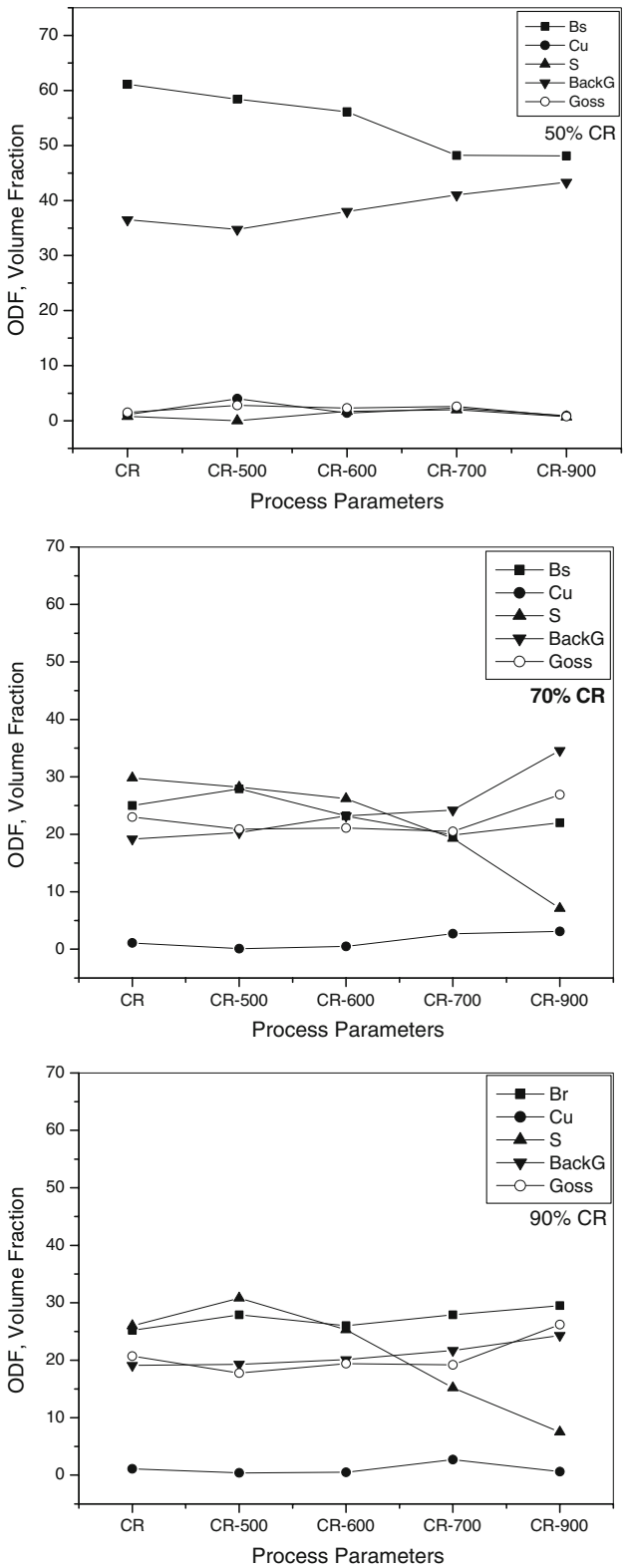

Fig. 4 Volume fractions of some of the major texture components of 316L SS

Table 1 Tensile properties of 316L SS obtained under different rolling and after annealing conditions

Process parameters	$YS_{0.2\%}$ (MPa)	% Elongation	Strain hardening exponent, *n*
Starting material	268	58	0.408
50% CR	986.43	11.41	0.009
50% CR + 500 °C	997.1	13.52	0.04
50% CR + 600 °C	667.7	17.75	0.063
50% CR + 700 °C	710.85	21.67	0.097
50% CR + 900 °C	277.98	45.2	0.218
70% CR	1089	11.97	Negligible
70% CR + 500 °C	1132	12.99	0.016
70% CR + 600 °C	964	16.99	0.05
70% CR + 700 °C	896.7	21.07	0.146
70% CR + 900 °C	279.69	45.3	0.414
90% CR	1205	7.02	Negligible
90% CR + 500 °C	1291	6.7	Negligible
90% CR + 600 °C	1101	9.39	0.04
90% CR + 700 °C	971	12.61	0.047
90% CR + 900 °C	321.62	46.00	0.387

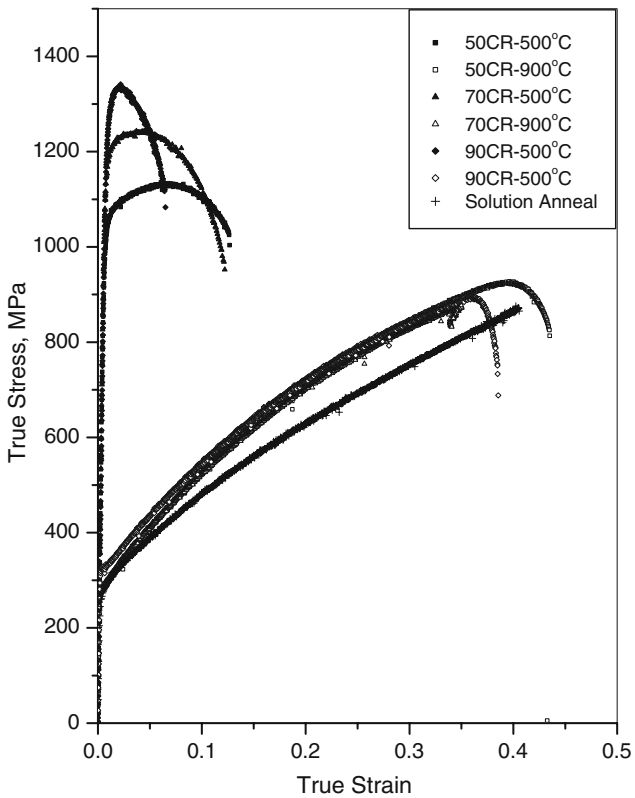

Fig. 5 The true stress–strain response of the cold rolled and annealed 316L ASS

in the decrease in yield strength by about 20–30% from the as-cold rolled condition. Very little improvement was found in the % of elongation. Further, annealing at 900 °C temperature considerably reduced the yield strength with corresponding major increase in the % of elongation. In general, the behaviour of the stress–strain curve was distinctly of two different natures. A drop in stress immediately after the peak stress was reached for specimens that retained cold deformed structure was seen. This exhibits very poor strain hardening ability of the ASS immediately after the yielding, indicating poor plastic deformation behaviour. This could be attributed to the severely deformed microstructure (Fig. 2) saturated with high dislocation density even after annealing treatment at and below 700 °C. On the other hand, small yield strength and good strain hardening ability during plastic deformation was noted for fully recrystallized ASS at 900 °C. Effect of strain hardening ability as a function of annealing temperature is also presented in Fig. 6. The strain hardening ability of the cold rolled ASS was very small at an annealing temperature of 700 °C and less. In general, strain hardening ability of the ASS increased with increasing annealing temperature. To gain greater insight in the tensile behaviour of the ASS, strain hardening rate, 'θ', is plotted against true stress as shown in Fig. 7. Strain hardening rate was determined through numerical differentiation of the stress–strain curve

$$\theta = \frac{d\sigma}{d\varepsilon} \tag{3}$$

The fluctuating feature of the curve is due to the differentiation of the experimental data. The plot showed distinctly different type of the behaviour in cold rolled conditions and after annealing. An initial increase in the strain hardening rate and then decrease with stress for fully recrystallized ASS was observed. This was then followed by an approximately constant hardening rate with increasing stress. Of the three different rolling % of reductions, 50% cold rolled ASS after annealing showed a very distinct sharp increase in the initial hardening rate. On the other hand, specimens with severely deformed structure revealed initial high strain hardening rate with continuously decreasing trend with stress.

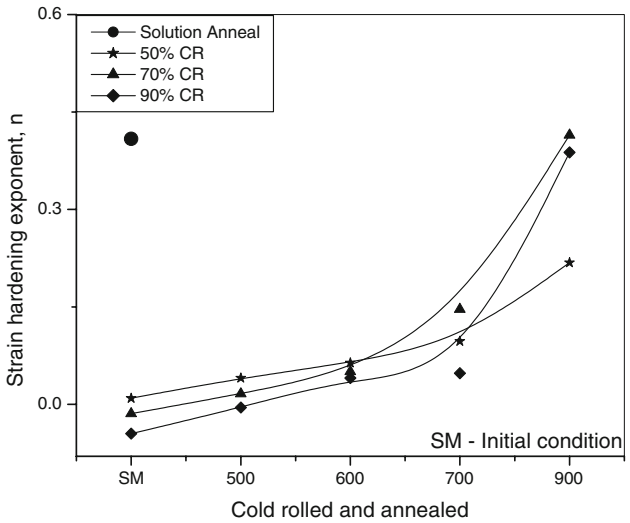

Fig. 6 Variation of strain hardening exponent '*n*' as a function of cold rolling and annealing of 316L SS

Effect of microstructure on mechanical properties

From observations on microstructural analysis, it was found that the cold deformed structure was retained even up to 800 °C. The full recrystallization of the cold deformed structure took place at an annealing temperature

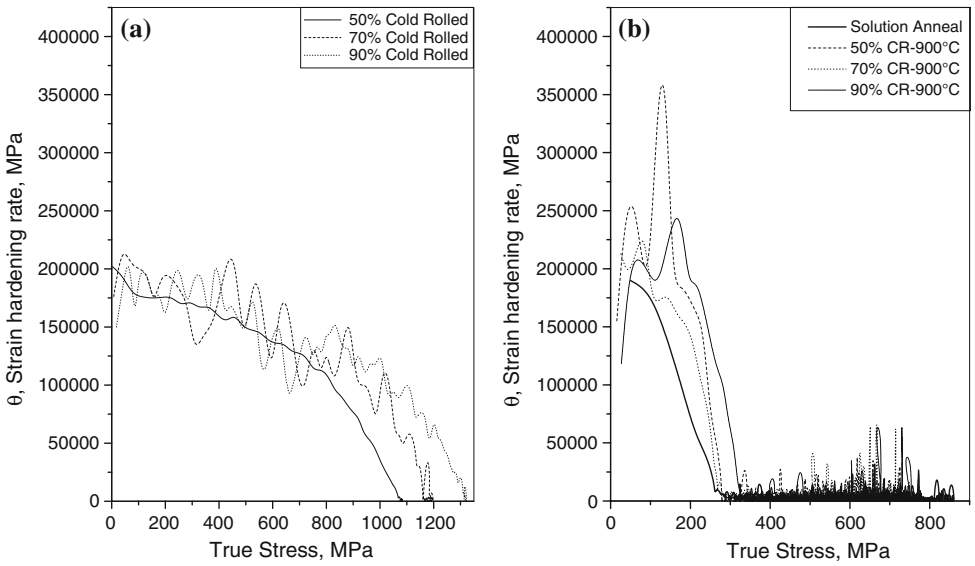

Fig. 7 **a** Strain hardening rate plotted against stress for cold rolled 316L SS, **b** annealed at 900 °C

of 900 °C with a very fine grain size. Therefore, below 900 °C, the ASS was composed of deformed microstructure, consisting of high dislocation substructure and cold rolling texture. The severity of deformed microstructure decreased with increasing annealing temperature up to 800 °C. Hence, the softening observed in the specimens was a contribution of microstructural changes (Table 1). At 900 °C, there was a large drop in the yield strength (~300) with a consequent increase in % elongation (~45). Di Schino et al. [15, 16] reported increase in the yield strength for austenitic stainless steels at grain size below ~4 μm. The grain size obtained in this study at 900 °C was about 6 μm that was very close to reported value. Thus, one may interpret that the little higher (~300 MPa) yield strength observed at 900 °C annealing of 90% cold rolled material could be a result of grain refinement. In essence, it may be concluded that the character of the microstructure greatly influenced the mechanical properties.

Effect of texture on Schmid factor and slip transmission number

Texture can influence two very important parameters: (a) Schmid factor 'θ' and (b) slip transmission number 'λ'. The type of texture evolved at thickness reduction of 50% and above was different in the ASS. At thickness reduction of 50%, development of a very strong $\{110\}\langle 112\rangle$B texture component was noted (Fig. 3). The presence of the B texture component orients $\{110\}$ plane parallel to the specimen sheet plane and $\langle 112\rangle$ direction parallel to the RD/tensile loading axis direction of the specimen. Similarly the other texture component observed at high % of cold rolling, $\{110\}\langle 001\rangle$G and $\{123\}\langle 643\rangle$S orientations, would result in the alignment of stress axis along $\langle 001\rangle$ and $\langle 643\rangle$ directions, respectively. Using the tensile stress directions, as determined from the B, G and S texture components, Schmid factor, 'μ', was calculated for critical resolved shear stress for the three texture components. The $\{111\}\langle 112\rangle$ slip systems of fcc lattice and all the possible variant selections of three B, G and S texture components were used for the Schmid factor calculations. A general trend in the 'μ' values generated for the three texture components is depicted in Fig. 8. All the three texture components show high to low Schmid factor. The G and S texture components' variants observed in this study were mostly associated with small 'μ' values (Fig. 8), whereas variants of B texture component mostly show high 'μ' values. Therefore, presence of grains with B orientation increases the probability of having high Schmid value.

Next we consider the effect of texture components on slip transmission number 'λ' according to Werner and Prantl [6]. The slip transmission number 'λ' for fcc/fcc grain boundaries, as the case in this study, generated by

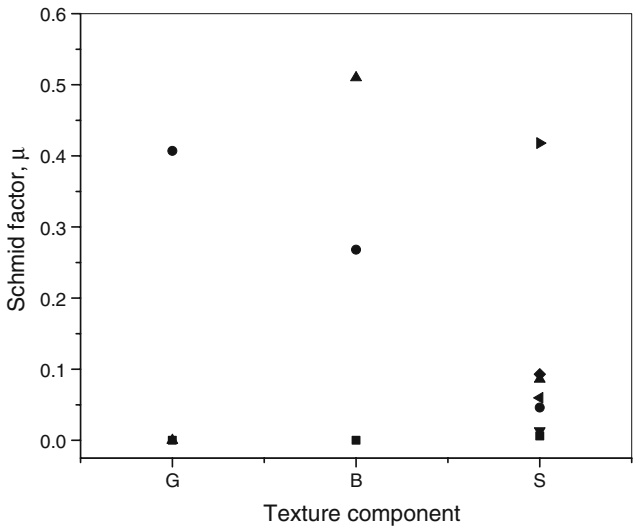

Fig. 8 Trends in the Schmid factor 'μ' values as a function of Goss (G), Brass (B) and S orientations for the fcc slip system $\{111\}\langle 112\rangle$. The different values of 'μ' represent for various variants of the G, B and S texture components

Werner and Prantl [6] was small (~2) for the B, G and S texture components. The small value of 'λ' was expected to hinder the slip transmission through grain boundaries. This was in turn expected to increase the yield strength of the material. However, a correlation between 'λ' and yield strength displayed contrary to the hypothesis.

From the above observations, it may be derived that the cold rolling textures developed in ASS lead to high 'μ' value (due to the presence of B texture component) and a small slip transmission numbers. Apart from these two factors, we have a third strongly influencing parameter in terms of microstructure. All these factors should contribute to enhance the tensile properties as discussed in preceding sections. Below 900 °C, the three parameters were collectively present in the material and therefore it was not possible to study the individual effect of these. However, it was possible to reduce/negate the contributions from microstructural parameters by annealing cold deformed structure at 900 °C, while retaining the entire texture components. Therefore, the tensile behaviour of the ASS annealed at 900 °C should reflect the contributions of texture alone in terms of Schmid factor and slip transmission number. A comparison amongst changes in yield strength and microstructure, Schmid factor and slip transmission number revealed that the yield strength was strongly dependent on the microstructural changes.

Figure 6 shows the strain hardening coefficient, 'n', as a function of process parameters. Our study revealed that this parameter was very small for cold rolled as well as after annealing below 900 °C. At 900 °C, this value was almost similar to ASS in solution anneal condition. However, the smallest value was noted for 50% cold rolled specimens

even after annealing at 900 °C. This was very interesting because similar fine-grained microstructure was displayed by all the other cold rolling conditions of ASS annealed at 900 °C. The possible explanation for observed small 'n' value of 50% cold rolled ASS may be the presence of very strong B texture component associated with high Schmid value, 'μ'. Slip systems in the grains with high value of 'μ' should be the first to get activated compared to the others during plastic deformation [6]. Thus, all grains with B orientation should result in simultaneous slip activity influencing strain hardening parameter. But insensitiveness of the 'n' parameter at higher % of cold reduction could not be explained by the above argument. Hence, 'n' may not be a very sensitive parameter to fully translate the effect of texture on tensile behaviour. The same could be observed for slip transmission number 'λ'.

Alternatively, we looked at the strain hardening rate of the ASS. Interestingly, it was found that this parameter translated the effect of texture and microstructure very vividly. In the presence of heavily deformed microstructure, the rate continuously decreased. On the other hand in the absence or less influence of microstructure, the rate increased initially and then sharply dropped. In the presence of strong B texture component, as in 50% cold rolled ASS, it showed very high strain hardening rate. This was an anticipated behaviour of the material with very high 'μ' value due to multiple slip activity. Unlike 'n' parameter, the effect of strain hardening rate was evident even for higher % of cold rolled and annealed ASS when compared with solution annealed ASS. Hence, the influence of Schmid factor and slip transmission number showed preferable influence on plastic deformation of the ASS compared to yield strength of the material as in the case of Hall–Petch relation.

Conclusions

The parameters related to grain orientation distribution were correlated with the tensile properties of the 316L SS in cold rolled and in cold rolled and annealed conditions.

(a) Through appropriate selection of annealing temperature, it was possible to fully recrystallize the heavily cold deformed microstructure, while retaining the crystallographic texture. The softening of 316L SS, despite the presence of strong cold rolling texture after annealing, indicated that the texture in this case does not influence the yield strength. The yield strength appears to be more influenced by the character of the microstructure rather than the type and magnitude of the texture.

(b) The texture/grain orientation was assessed in terms of their efficacy to rendering grain boundaries as an obstacle to slip transmission. Slip transmission number 'λ' for all the developed three texture components resulted in a small value. It was expected that the small value would expected to increase the resistance of grain boundaries to slip transmission. However, its influence on the yield strength was almost negligible. Further, a conclusive influence of this parameter could not be realized in this investigation due to synergistic effect of the Schmid factor.

(c) A strong influence of the texture components could be seen in terms of Schmid factor resulting into multiple slip activity. This was more predominant for B texture component.

(d) In this investigation, strain hardening rate, 'θ', was found to be a more sensitive parameter for revealing the influence of texture alone on tensile deformation behaviour compared to strain hardening coefficient 'n'.

Acknowledgements The authors are grateful to Professor S.P. Mehrotra, Director, National Metallurgical Laboratory, for supporting this study. The authors also thank Sri P.K. De for helping in various experiments, and M/s Salem Steel plant, India, for providing the material for this study.

References

1. Hingwe AK, Subramanian KN (1975) J Mater Sci 10:183. doi:10.1007/BF00540340
2. Ashmawi WM, Zikry MA (2002) Trans ASME 124:88
3. Ashmawi WM, Zikry MA (2003) Mater Sci Eng A 343:126
4. Honeycombe RWK (1968) The plastic deformation of metals. Edward Arnold, London
5. Gironès A, Vallechaise P, Mateo A, Anglada M, Mèndez J (2004) Mater Sci Eng A 387–389:516
6. Werner E, Prantl W (1990) Scr Mater 38:533
7. Le TC, Robertson IM, Birnbaun HK (1992) Acta Mater 40:2569
8. Schulz LG (1949) J Appl Phys 20:1030
9. Pawlik K, Ozga P (1999) LaboTex: the texture analysis software. Göttinger Arbeiten zur Geologie und Paläontologie, SB4
10. Pawlik K (1986) Phys Status Solidi B 134:477
11. Hirsch J, Lucke K (1988) Acta Mater 36:2863
12. Zhou Y, Tóth LS, Neale KW (1992) Acta Mater 40:3179
13. Ray RK, Jonas JJ, Hook RE (1994) Int Mater Rev 39:129
14. Donadille C, Valle R, Dervin P, Penelle R (1989) Acta Mater 37:1547
15. Di Schino A, Salvatori I, Kenny JM (2002) J Mater Sci 37:4561. doi:10.1023/A:1020631912685
16. Di Schino A, Barteri M, Kenny JM (2003) J Mater Sci 38:4725. doi:10.1023/A:1027470917858